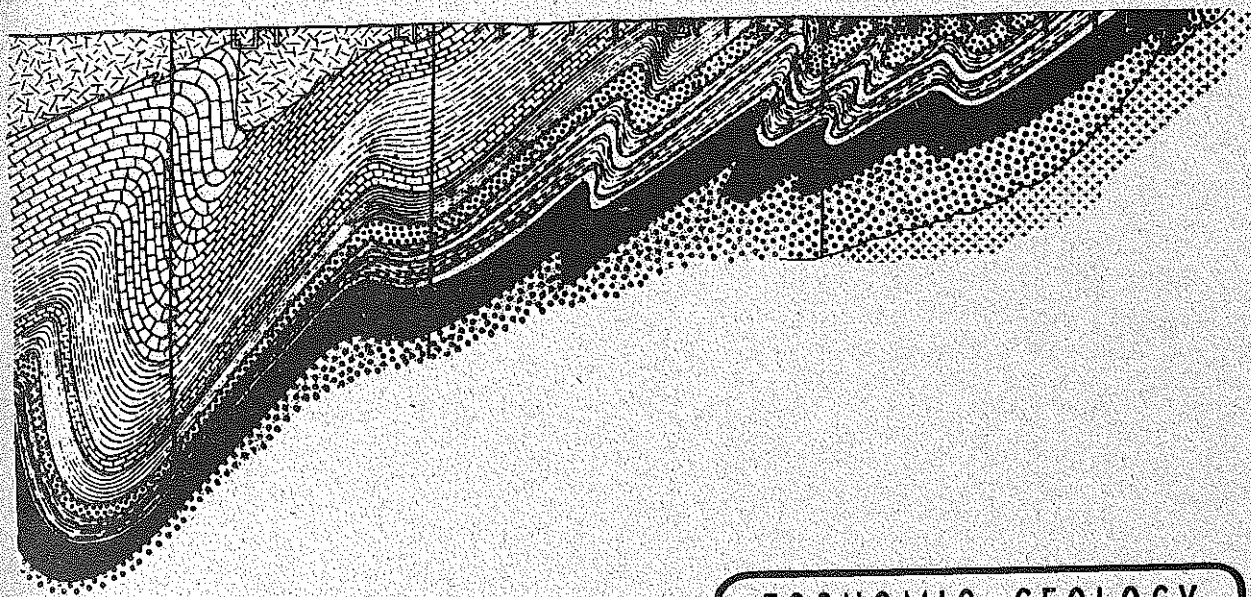




UNIVERSITY OF THE WITWATERSRAND  
JOHANNESBURG



ECONOMIC GEOLOGY  
RESEARCH UNIT

INFORMATION CIRCULAR # 7

UNIVERSITY OF THE WITWATERSRAND

JOHANNESBURG

THE USES AND LIMITATIONS OF  $\beta$  DIAGRAMS AND  
 $\pi$  DIAGRAMS IN THE GEOMETRICAL ANALYSIS  
OF FOLDS

by

J.G. RAMSAY

Visiting Specialist in Structural Geology  
from the  
Imperial College of Science and Technology, London,  
in the  
Economic Geology Research Unit

INFORMATION CIRCULAR NO. 7

JUNE, 1962

INFORMATION CIRCULAR NO. 7

(For Restricted Distribution)

The information contained herein is to be submitted for publication in a recognized journal and is made available on the understanding that extracts or references may not be published prior to publication of the original without the consent of the author.

## FORWARD

During the period May-September, 1961, Dr. John G. Ramsay, of the Imperial College of Science and Technology, London, was actively associated with the Economic Geology Research Unit in the capacity of a visiting specialist in structural geology. He participated in the three research projects then in progress - specialized studies of the Damara System in South West Africa, the Witwatersrand System in the Transvaal and Orange Free State, the Basement Complex in the Barberton Mountain Land, Eastern Transvaal.

One of the major aspects of these specialized studies involves attempts to decipher the tectonic style imposed upon these formations. Of particular importance is the necessity to unravel the pattern of folding and to define the axes of such folds. In areas where outcrops are poorly developed and it is out of the question to delineate the hinge zones of the folds, these axes have been determined by measuring the orientation of bedding planes and then analysing such data by means of  $\beta$  diagrams and  $\pi$  diagrams. Such an approach was used in mapping the folded Witwatersrand sediments in the Heidelberg and West Rand areas.

This Information Circular represents a critical assessment of the validity of employing such methods and, consequently, is of direct application to the structural studies currently being undertaken by the Unit.

D.A. PRETORIUS  
Senior Research Fellow

THE USES AND LIMITATIONS OF  $\beta$  DIAGRAMS AND  $\pi$  DIAGRAMS  
IN THE GEOMETRICAL ANALYSIS OF FOLDS

ABSTRACT

The two standard procedures for determining the direction of fold axes from measurements of the orientation of planar surfaces in the fold are examined to determine the validity of the conclusions which are generally based on them. With some types of folds, an analysis of the data using a  $\beta$  diagram gives results which are particularly difficult to interpret with any precision. Great errors in the position of the significant  $\beta$  intersections may be expected under certain circumstances, and geologically meaningless  $\beta$  points may also be abundant. Where the folding is inhomogeneous,  $\beta$  diagrams generally produce a particularly high proportion of spurious  $\beta$  points often greatly outnumbering the significant  $\beta$  points. Under these circumstances  $\beta$  diagrams are most unreliable and may give a false impression of the structural geometry. The most satisfactory method of analysing field data is by using the  $\pi$  diagram. Although there may be some difficulties in their interpretation when used with certain types of fold, modifications of the method may be employed to determine accurately the axes of both very open and near isoclinal folds. If  $\pi$  diagrams are prepared from data collected in regions of inhomogeneous folding, the inhomogeneities are often immediately apparent enabling the region to be subdivided into smaller areas of greater homogeneity. No mass of spurious points will be produced in such circumstances as would be found in a  $\beta$  diagram prepared from the same data.

THE USES AND LIMITATIONS OF  $\beta$  DIAGRAMS AND  $\pi$  DIAGRAMS  
IN THE GEOMETRICAL ANALYSIS OF FOLDS

CONTENTS

	Page
I. Introduction	1
II. $\beta$ Diagrams Prepared from Data Collected in Regions of Homogeneous Homoaxial Folding	1
(a) Errors in the Positions of Significant $\beta$ Points	4
(b) Development of Spurious $\beta$ Intersections	4
III. $\beta$ Diagrams Prepared from Data Collected in Regions of Single Phase Inhomogeneous Folding or in Regions of Superimposed Folding	6
IV. $\pi$ Diagrams Prepared from Data Collected in Regions of Homogeneous Homoaxial Folding	11
V. $\pi$ Diagrams Prepared from Data Collected in Regions of Inhomogeneous Folding	13
VI. Conclusions	13
VII. References	14

Enclosed: four diagrams plus explanations  
of text figures

THE USES AND LIMITATIONS OF  $\beta$  DIAGRAMS AND  $\pi$  DIAGRAMS  
IN THE GEOMETRICAL ANALYSIS OF FOLDS

INTRODUCTION

The structural geologist often finds it necessary to determine the orientation of the axis of folding with some precision. Several methods have been evolved by which measurements made during a field investigation may be employed to determine the direction and angle of plunge of the fold axis in that region. The two most commonly used graphical methods by which this is done both use stereographic constructions and lead to the production of what are known as  $\beta$  diagrams and  $\pi$  diagrams. Although these methods are generally well known, few people seem to have discussed the practical difficulties involved in their construction, or the validity of the deductions made from them. Discussions with other workers engaged on research problems in structural geology have suggested that there is some widespread concern about the validity of the analytical techniques employed in some recent publications. The author would like to acknowledge in particular the most useful discussions he had with C. Roering of the Economic Geology Research Unit, University of the Witwatersrand, in this respect.

In this paper both types of construction will be examined to determine their practical limitations in regions of single phase homogeneous cylindroidal folding and also in regions of single phase or poly-phase inhomogeneous folding.

$\beta$  DIAGRAMS PREPARED FROM DATA COLLECTED IN REGIONS OF HOMOGENEOUS  
HOMOAXIAL FOLDING

The axis of a fold should coincide with the lines of intersection of all bedding and schistosity (cleavage) surfaces generated by the fold movements. Sander (1948) pointed out how this geometric principal could be used to determine the orientation of the fold axis: if the orientation of the bedding planes at localities A and B on a fold (figure 1) are known, their intersection (known as a  $\beta$  axis) can be calculated and this line will be parallel to the fold axis, f. Similarly, the intersection of the bedding surface measured at locality B with the cleavage measured at locality C is another  $\beta$  axis. All axes calculated in this way should be parallel, but because the folding is rarely perfectly homoaxial and because measurements of bedding planes are always subject to a certain error, the  $\beta$  axes do not all coincide but group around a mean value. The most practical method for graphi-

cally computing the  $\beta$  intersections employs an equal area (Schmidt) stereogram in the following way:-

- (1) Plot the great circle representing one of the observed surfaces.
- (2) Plot a second great circle representing another plane and determine the point of intersection ( $\beta$  axis) with the first great circle.
- (3) Plot successive great circles representing other observed bedding planes and determine their intersections with all other great circles.

The number of  $\beta$  intersections produced by  $x$  observed planes is the sum of the arithmetic progression:-

$$0 + 1 + 2 + 3 + \dots + (x-1) \text{ i.e. } \frac{x(x-1)}{2} \dots (1)$$

The first practical limitation of  $\beta$  diagrams can be seen from the nature of this formula. The number of  $\beta$  intersections outnumbers the number of observations if  $x > 3$ , particularly when  $x > 10$ . This means that, if many observations have been made at one locality, it is often very difficult, or even impossible, in practice to combine them into a single diagram (e.g. if  $x = 200$ ,  $\beta = 19,900$ ). In such instances the data from the region must be divided into smaller sub-areas (say  $x=15$  then  $\beta = 105$ ). The impressively large number of  $\beta$  points and  $\beta$  diagrams which may be obtained from relatively few primary observations sometimes tends to overimpress the investigator and give a false sense of accuracy.

When the points have been plotted, the vector mean must be determined and various methods may be employed depending on the required degree of precision:-

- (1) It is sometimes possible to establish the centre of concentration of the  $\beta$  group by inspection.
- (2) The centre of concentration may be determined by using a contouring counter (see Knopf and Ingerson, 1938, p.24, 245-251).
- (3) If the  $\beta$  vectors are unimodal, the mean vector may be determined by first measuring the angle between each axis and three perpendicular co-ordinate axes (for convenience N - S horizontal, E - W horizontal, and verti-



cal)  $\Psi_1, \Psi_2$  and  $\Psi_3$  respectively (see figure 2), then using the formula for the mean direction cosines:-

$$\cos \bar{\Psi}_1 = \frac{\sum \cos \Psi_1}{\sqrt{(\sum \cos \Psi_1)^2 + (\sum \cos \Psi_2)^2 + (\sum \cos \Psi_3)^2}} \quad (2)$$

$$\cos \bar{\Psi}_2 = \frac{\sum \cos \Psi_2}{\sqrt{(\sum \cos \Psi_1)^2 + (\sum \cos \Psi_2)^2 + (\sum \cos \Psi_3)^2}} \quad (3)$$

$$\cos \bar{\Psi}_3 = \frac{\sum \cos \Psi_3}{\sqrt{(\sum \cos \Psi_1)^2 + (\sum \cos \Psi_2)^2 + (\sum \cos \Psi_3)^2}} \quad (4)$$

Although it is only necessary to calculate  $\bar{\Psi}_1$ , and  $\bar{\Psi}_2$  the third calculation provides a good arithmetic check.

The advantages of this last method are its precision and the possibility of further statistical work (calculation of the standard deviation from the mean etc.). The disadvantages are the amount of work involved in measuring the angles  $\Psi_1, \Psi_2$  and  $\Psi_3$  for the calculations, particularly if the number of  $\beta$  points is very large.

Until now little account has been taken of the effects of possible errors in the field observations. It is rarely possible, with the equipment normally used by geologists, to measure surfaces to the precision of a degree or even several degrees. The errors inherent in the primary data lead to two types of error in  $\beta$  diagrams:-

- (1) Error in the position of the true significant  $\beta$  intersections.
- (2) Error arising from the development of spurious  $\beta$  intersections having no geological significance whatsoever.

Since these two effects may make  $\beta$  diagrams prepared from field data difficult to interpret, often the practical use of this method of fold analysis is severely limited. These two types of error in the positions will now be examined in more detail.

### (a) Errors in the Position of Significant $\beta$ Points

Let us consider the effects of an error in measurement of two bedding planes with poles A and B (figure 3), located in a homogeneous cylindroidal fold (Clark and McIntyre, 1951) and where the angle between the planes is  $d$ . If these planes could be measured exactly, it would be possible to construct their intersection ( $\beta$ ); but this is not possible and we must examine the effects of a possible maximum error of  $e_\pi$  degrees in these observations, such that the poles of the measured surfaces A and B will fall somewhere within the small circles at distances  $e_\pi$  degrees from their true positions. The range of error in the position of the  $\beta$  intersection of these two planes lies in the stippled area delimited in figure 3; the  $\beta$  point will lie somewhere within the spaces enclosed by the intersection of two cones with apical angles of  $(90 - e_\pi)$  degrees and with axes positioned at an angle  $d$  degrees apart. In figure 4 the poles of the two surfaces have been changed to positions  $A^1$  and  $B^1$  so that the angle between them is decreased to  $d^1$ . The range of error  $e_\beta$  in the position of the intersection as the result of an error  $e_\pi$  in the position of  $A^1$  and  $B^1$  is now much greater. The maximum error in the position of the  $\beta$  point ( $\max e_\beta$ ) clearly depends on two factors, the amount of maximum error in  $e_\pi$ , and the angle  $d$  between the two planes. Graphs showing the amount of maximum error  $e_\beta$  for various values of  $e_\pi$  and  $d$  are shown in figure 5. The maximum error  $e_\beta$  is greatest where the angle between the surfaces is small, and in consequence the  $\beta$  diagram method of fold analysis is particularly unsatisfactory where the folds are of a gentle, open type or where they are of a tight isoclinal type.

As the angle  $d$  between the planes becomes smaller, the  $\beta$  axes tend to spread along a great circle, the pole of which bisects the poles A and B (figure 4).  $\beta$  diagrams made from data taken from areas where the planar structures show no great angular variation often show this tendency for the  $\beta$  points to be dispersed along a great circle (Weiss, 1954; Lindstrom, 1961 b). This arrangement has no particular geological significance, but results inevitably from the geometrical nature of the data combined with errors in measuring the surfaces. If such diagrams are to be interpreted, it appears that only the main  $\beta$  maximum within the great circle has any significance.

### (b) Development of Spurious $\beta$ Intersections

If the measurement of any one surface is subject to an error, then the  $\pi$  poles of a number of measurements taken on a series of perfectly plane surfaces will form a group about the true position

A (figure 6). If a  $\beta$  diagram is prepared from a group of observations such as this, even though there is no axis of folding, the  $\beta$  points will scatter in a small circle zone (i.e. within a conical space of apical angle  $90 - e_{\pi}$  degrees). Although this scatter of points has no geological significance whatsoever, spurious  $\beta$  points that arise in this manner are likely to occur in most  $\beta$  diagrams prepared from field data, and there is often no practical method by which they may be differentiated from significant  $\beta$  intersections. These spurious  $\beta$  intersections will be particularly abundant in a diagram prepared from folds where the bedding planes show a strong preferred orientation, where the folds are of a gentle, open type (figure 11, 1) or of a tight isoclinal type (figure 11, 3), where the folds have well developed limbs (figure 11, 2B), or where many measurements of sub-parallel axial plane cleavages are incorporated into the  $\beta$  plot. Under certain of these circumstances, the number of spurious intersections may exceed the number of geologically significant  $\beta$  points, and as has been discussed above, these significant points are also subject to positional error. It has been argued that the errors which may arise tend to be randomly distributed, whereas the significant  $\beta$  intersections concentrate about a mean position (Lindstrom, 1961). The errors are not, however, distributed in a completely random fashion, the significant  $\beta$  intersections spread along a great circle zone, and the spurious readings concentrate in small circle zones. With gentle, open folds and with isoclinal folds these scatter distributions tend to coincide and it is often possible to obtain maxima and sub-maxima in the compound scatter zone by chance alone.

With homogeneous cylindroidal fold systems the  $\beta$  diagram method of fold axis determination is limited in its application. It seems only advisable to use it where the angles between the bedding planes vary from 40 degrees to 140 degrees, and where the bedding planes show a considerable range in orientation and the folds have rounded hinges.

If useful  $\beta$  diagrams are to be prepared from field data it is most important to make the field measurements with the maximum possible accuracy. Where the beds are slightly or isoclinally folded it is unlikely that this can be done with sufficient precision using only a field geologist's compass.

$\beta$  DIAGRAMS PREPARED FROM DATA COLLECTED IN REGIONS OF SINGLE PHASE  
INHOMOGENEOUS FOLDING OR IN REGIONS OF SUPERIMPOSED FOLDING

In regions of single phase homogeneous folding it has been shown that, although there may be practical difficulties involved in both the construction and interpretation of details of  $\beta$  diagrams prepared from such terrain, the main  $\beta$  maximum is generally parallel to the axes of the folds. A further interpretation of these diagrams has been developed. It has been suggested that where several maxima of  $\beta$  are developed, these represent the axes of several co-existing fold directions, and that the intensity of the various maxima and sub-maxima is to be directly correlated with the intensity of development of the various fold systems (Weiss, 1954; Fleuty, 1962).

Extensive investigations have been carried out on the various phases of folding seen in the Moinean rocks of the Caledonian fold belt in the Northern Highlands of Scotland. At an early stage in this work it became of importance to ascertain the methods by which the various geometrical elements of the interfering fold systems could be accurately determined. In this terrain it became apparent that some of the methods of structural analysis of the field data gave consistent and satisfactory results, while others proved to be partly inadequate. The  $\pi$  diagram method and modifications of it, to be described in a later section of this paper, were found to offer the most reliable way for the determination of many features of the fold geometry. The technique of determining the various sets of fold axes by the  $\beta$  diagram method proved to be generally unworkable, and on further investigation there seems to be clear reasons why it is, in fact, mathematically unsound.

Lindström has recently published the results of several structural investigations in parts of the Caledonides of Scandinavia (1961 b) where he recognises several phases of folding. He has revived and considerably developed the technique of interpreting the various maxima and sub-maxima seen in  $\beta$  diagrams, and he has suggested that these methods offer the most sensitive way of discovering the different fabric elements in an area of deformed rocks (1960; 1961 a; 1961 b). However, these techniques would appear to be fundamentally unsound, and although they may give correct results in some areas they are not of general application on account of their inherent fallacies. The intrinsic fallacy is contained in Lindström's statement (1961, p.351), "Each  $\beta$  intersection is potentially a fold axis". This idea is now examined in some detail in order to develop a mathematical basis for the numbers of  $\beta$  points and of their significance in regions of several directions of folding.

In regions which have suffered two phases of deformation,

folds with many different orientations may have been produced, and although the minimum number of principal trends is four, there may be many other subsidiary directions. In the area in which a certain amount of field data has been accumulated there are, say,  $n$  fold axis directions. If it were possible to subdivide the data and to apportion the various field observations to their respective fold directions it would be possible to make  $n$  diagrams and determine the various axes of folding (figure 7). In practice this is impossible, and a single  $\beta$  diagram is constructed which combines all the available data. This means that surfaces which are related to folding about one axis are combined with surfaces related to another axial direction to produce  $\beta$  intersections which are not parallel to any fold axis, they are spurious points with no geological significance. There is no practical way by which the genuine readings may be distinguished from the spurious. It is possible to compute the number of genuine and spurious  $\beta$  intersections if the number of fold systems is known, and if the way the data is distributed through the fold systems is also known:

Let the total number of observations of planar surfaces be  $x(c_1 + c_2 + c_3 + \dots + c_n)$  distributed through  $n$  fold systems  $f_1, f_2, f_3, \dots, f_n$  in the manner shown in figure 7, where  $c_1, c_2, c_3, \dots, c_n$  are constants such that  $c_1x, c_2x, c_3x, \dots, c_nx$  are positive integers and  $1 \leq c_1 \leq c_2 \leq c_3 \leq \dots \leq c_n$ . From (1) the total number of significant  $\beta$  intersections in a diagram constructed from all the data is:

$$\begin{aligned} \beta \text{ sig} &= \frac{c_1x(c_1x-1)}{2} + \frac{c_2x(c_2x-1)}{2} + \dots + \frac{c_nx(c_nx-1)}{2} \\ \beta \text{ sig} &= \frac{x^2 \sum_{i=1}^n c_i^2}{2} - \frac{x \sum_{i=1}^n c_i}{2} \quad (5) \end{aligned}$$

The total number of spurious  $\beta$  intersections resulting from combining data from  $f_1$  with that from  $f_2, f_3, f_4, \dots, f_n$ , and data from  $f_2$  with that from  $f_3, f_4, \dots, f_n$  etc. is

$$\begin{aligned} \beta \text{ spu} &= c_1x(c_2x + c_3x + \dots + c_nx) + c_2x(c_3x + c_4x + \dots + c_nx) + \dots \\ &\quad + c_{n-2}x(c_{n-1}x + c_nx) + c_{n-1}xc_nx \\ \beta \text{ spu} &= x^2 \sum_{y=1}^{n-1} c_y(c_{y+1} + c_{y+2} + \dots + c_n) \quad (6) \end{aligned}$$

The number of spurious  $\beta$  points in the total

$$\frac{\beta_{sig}}{\beta_{spu} + \beta_{sig}} = \frac{2x \sum_{y=n-1}^{y=1} c_y (c_{y+1} + c_{y+2} + \dots + c_n)}{x \left[ 2 \sum_{y=n-1}^{y=1} c_y (c_{y+1} + c_{y+2} + \dots + c_n) + \sum c_n^2 \right] - \sum c_n} \quad (7)$$

Similarly the number of genuine  $\beta$  points in the total

$$\frac{\beta_{sig}}{\beta_{spu} + \beta_{sig}} = \frac{x \sum c_n^2 - \sum c_n}{x \left[ 2 \sum_{y=n-1}^{y=1} c_y (c_{y+1} + c_{y+2} + \dots + c_n) + \sum c_n^2 \right] - \sum c_n} \quad (8)$$

Equations (7) and (8) are of the form

$$F = \frac{Ax}{Bx - C} \quad \text{and} \quad F = \frac{Dx - C}{Bx - C} \quad \text{respectively}$$

where A, B, C and D are constants of positive value where  $B > A > D > C$ .

$$\frac{dF}{dx} = - \frac{AC}{(Bx - C)^2} \quad \text{and} \quad \frac{dF}{dx} = 0 \quad \text{when } x = \infty$$

$$\frac{d^2F}{dx^2} = \frac{2ABC}{(Bx - C)^3} \quad \text{and is positive for all positive values of } x.$$

where  $x = \infty$  the value for F is a minimum.

$$\frac{dF}{dx} = \frac{BC - DC}{(Bx - C)^2} \quad \text{and} \quad \frac{dF}{dx} = 0 \quad \text{when } x = \infty$$

$$\frac{d^2F}{dx^2} = \frac{2BC(D - B)}{(Bx - C)^3} \quad \text{and is negative for all positive values of } x.$$

where  $x = \infty$  the value for F is a maximum.

therefore as  $x \rightarrow \infty$  equation (7) approaches the minimum value

$$\frac{2 \sum_{y=n-1}^{y=1} c_y (c_{y+1} + c_{y+2} + \dots + c_n)}{2 \sum_{y=n-1}^{y=1} c_y (c_{y+1} + c_{y+2} + \dots + c_n) + \sum c_n^2} \quad (9)$$

and equation (8) approaches the maximum value

$$\frac{\sum c_n^2}{2 \sum_{y=n-1}^{y=1} c_y (c_{y+1} + c_{y+2} + \dots + c_n) + \sum c_n^2} \quad (10)$$

Putting  $c_1 = c_2 = c_3 = \dots = c_n = 1$  in (10) the maximum number of significant intersections in the total is  $\frac{1}{n}$

Thus if the data is equally distributed throughout the  $n$  fold systems, the maximum proportion of significant  $\beta$  points in the total can never exceed  $\frac{1}{n}$ .

It is not possible to describe in any simple way the effects of all possible variations of  $c_1, c_2, c_3, \dots, c_n$  on the proportions of significant  $\beta$  points in the total, but it is possible to obtain some impression of these effects by considering the effect of dispersing the data so that  $c_1 = 1$ , and  $c_2 = c_3 = c_4 = \dots = c_n = c$ . From (9) the maximum value of

$$\frac{\beta_{\text{sig}}}{\beta_{\text{total}}} \text{ is } \frac{c^2(n-1) + 1}{[c(n-1) + 1]^2} \dots \dots \dots (11)$$

The variations in this value depending on the values of  $c$  and  $n$  are graphically recorded in figure 8. From these graphs it can be seen that as the data become more unequally dispersed through the fold systems, so the number of significant  $\beta$  readings in the total becomes larger.

Although the number of significant readings in the total increases, let us examine the number of the significant  $\beta$  points from the least well developed fold systems and compare them with the number of spurious points:

$$\frac{\beta_{\text{spu}}}{\beta_{\text{from } f_1}} = \frac{2x \sum_{y=n-1}^{y=1} c_y (c_{y+1} + c_{y+2} + \dots + c_n)}{c_1^2 x - c_1} \quad (12)$$

as  $x \rightarrow \infty$  this approaches a minimum value of

$$\frac{2 \sum_{y=n-1}^{y=1} c_y (c_{y+1} + c_{y+2} + \dots + c_n)}{c_1^2} \quad (13)$$

and with the conditions  $c_1 = 1$ , and  $c_2 = c_3 = c_4 \dots = c_n = c$   
the minimum value is:

$$2c(n-1) + c^2(n-2)(n-1) \dots \dots \dots (14)$$

This function is graphically recorded in figure 9, and the following facts are clearly illustrated:

- (1) There will always be at least twice as many spurious  $\beta$  intersections as significant  $\beta$  points related to the least well developed fold systems.
- (2) If there are several axes of folding the significant intersections from the least well developed fold systems are almost certain to remain undetected in the masses of geologically meaningless  $\beta$  points.

These conclusions regarding the maximum number of significant axes and the minimum number of spurious  $\beta$  intersections have been reached assuming ideal  $\beta$  plots, and the values graphically recorded in figures 8 and 9 can never be exceeded in practice. They are in fact only rarely approached, because when  $\beta$  diagrams are prepared it is not technically possible to incorporate a large number of observations. Yet another feature which leads to even less satisfactory results than these graphs suggest is the type of position error in the significant  $\beta$  points resulting from errors in the field measurements as described previously.

From these calculations it can be seen that  $\beta$  diagrams are particularly unreliable in regions where the folding is not homogeneous, and that the interpretation of the various sub-maxima that may appear is never a simple routine matter. In some geological circumstances the spurious  $\beta$  intersections will tend to scatter in a random fashion whereas the significant  $\beta$  points tend to concentrate, but much depends upon the shapes of the various fold systems. Thus the significant data will tend to scatter if the angles between the limbs of any of the fold sets is less than about 40 degrees or greater than 140 degrees. If the folds which are oriented in various directions show certain preferred orientations of bedding planes (e.g. if they have well developed limbs), then it is possible to produce concentrations of spurious  $\beta$  points from the intersection of planes from the limb of one fold from those of another.



Lindstrom (1961 b) has described another type of  $\beta$  synopsis which may be produced by combining only the data from any two adjacent surfaces. This would certainly be an improvement on the normal  $\beta$  synopsis and would tend to reduce the numbers of spurious intersections that arise by combining surfaces related to one fold system with those from another. However, if the ratio of the fold wavelength to the distance between the observations is large, the angle between the adjacent planes is likely to be small and this means that the errors in position of the significant  $\beta$  points as computed in figure 5 are likely to be large.

#### $\pi$ DIAGRAMS PREPARED FROM DATA COLLECTED IN REGIONS OF HOMOGENEOUS HOMOAXIAL FOLDING

The principal on which the so-called  $\pi$  diagrams are prepared is a simple one (Sander, 1948). At any series of points A, B, C and D on a fold (figure 10) the orientations of bedding planes are measured and the normals to these surfaces (known as  $\pi$  poles) are constructed. These  $\pi$  poles all lie on a plane or series of parallel planes oriented normal to the fold axis. The normals to the cleavage surfaces or axial planes of the folds (E in figure 10) are also contained in the same series of parallel planes. These constructions are most simply made with a stereogram: the  $\pi$  poles are plotted and fall on or about one particular great circle, the pole of which is parallel to the fold axis f.

The advantages of this method of analysing field data over the diagram method are very considerable:-

- (1) Large numbers of  $\pi$  poles can be plotted in one diagram (several thousand if necessary), and these diagrams are, as a result, of far greater statistical accuracy than the  $\beta$  diagrams. The unwieldly quadratic rate of increase of  $\beta$  points with increasing numbers of field observations is avoided, and each field observation results in a single plot.
- (2) Inevitable errors in the field observations do not lead to the production of spurious data as with a  $\beta$  diagram.
- (3) More information about the folding can be obtained from a  $\pi$  diagram than from a  $\beta$  diagram. It is often possible to determine the profile shape of the folds, the angular relationships of the various planar structures in the folds, and, with certain types of folds, it may be possible to

measure the relative thinning and thickening of the strata on the fold limbs.

Although the  $\pi$  diagram offers a more reliable method of determining the fold axes than does the  $\beta$  diagram method, it does have some practical limitations with certain types of folds, if used in its simplest form. Figure 11 shows a series of folds of different styles and the  $\beta$  and  $\pi$  diagrams which can be prepared from data collected from them. Where the spread of the  $\pi$  poles is of the range 40 degrees to 140 degrees, it is a simple matter to determine the fold axis, but where the folds are open (type 1) or tight (type 3) there may not be sufficient spread of the  $\pi$  poles to locate accurately the great circle on which they lie. If the folding is isoclinal, the great circle may be more accurately placed if measurements of the bedding planes have been recorded at the hinge of the folds. Careful search is often necessary to find surfaces with this particular orientation. Without these measurements it may still be possible to determine the fold axis in the following way. The axial planes of the folds are constructed and the  $\pi$  poles from the two fold limbs are plotted on the same stereogram, but with different symbols. The poles should form two groups which may overlap depending on the angle between the fold limbs and the amount of error in the measurements of the surfaces *e.* The centres of concentration of the two groups are determined by using a contouring counter, or more accurately by employing the formulae (2), (3) and (4) to calculate the mean direction cosines. A great circle is then drawn through the two mean values and its pole will be parallel to the axis of folding. In strongly folded rocks this modification of the  $\pi$  diagram often proves to be particularly valuable (Ramsay, 1958 b, figure 7). A large number of observations can be used in the construction, and the more measurements employed the greater the accuracy of the work, whereas if this amount of data is used in a  $\beta$  diagram it produces a confusing zone of  $\beta$  intersections from which it is difficult or impossible to locate the main maximum (figure 11,  $\beta$  diagrams for folds of type 1 and 3).

When the  $\pi$  poles are plotted on a stereogram it will generally be found that they are located on only a part of a great circle; the angular spread of the  $\pi$  poles is directly related to the angle between the fold limbs and gives a measurement of the tightness of the fold (see figure 11). The  $\pi$  poles are sometimes not equally distributed within this partial great circle and there may be areas in which they concentrate. These concentrations might be the result of the nature of the exposures in the field, but they may have some more fundamental relationship to the shape of the folds. If there is a variation in the degree of exposure at different parts of the folds, then the sample of observations through the structure will not be statistically uniform. If the sample distribution is known to be

reasonably uniform the  $\pi$  pole concentrations must be related to planar structures which show a certain degree of preferred orientation as in folds with well developed limbs (see figure 11, type 2B). If the mean points around which the poles concentrate can be determined, these will give a measure of the average orientation of the fold limbs.

Certain types of fold, in particular those described as 'similar' folds, often show regularly oriented axial planes, and in folds of this type the beds vary in thickness as a result of deformation during the formation of the folds. If the axial planes of these folds bisect the angle between the fold limbs, the relative thickness of the beds in the fold limbs will be the same; if the axial planes do not bisect the angle between the fold limbs, the beds in one limb are thinned relative to the other. The ratio of thickness of any particular bed seen at different parts of the structure is related to the angle between the axial plane and the bedding such that:-

$$\frac{t}{T} = \frac{\sin \theta}{\sin \phi} \quad (\text{see figure 12})$$

#### $\pi$ DIAGRAMS PREPARED FROM DATA COLLECTED IN REGIONS OF INHOMOGENEOUS FOLDING

$\pi$  diagrams prepared from this data all show a scatter of  $\pi$  poles and they are no longer positioned on one great circle. Where there are two directions of folding it may be possible to discover two great circles which pass through the  $\pi$  poles, but it is generally more satisfactory wherever possible to subdivide the area into more homogeneous units and to make separate  $\pi$  plots for these sub-areas. For examples of the practical application of this technique in the complexly folded parts of the Caledonian fold belt of the Northern Highlands of Scotland the reader is referred to Johnson, 1957; Weiss and McIntyre, 1957; Ramsay, 1958 a, 1958 b; Clifford, 1960; and Fleuty, 1962. These techniques give more satisfactory results than the  $\beta$  diagram method since no spurious points ever appear on the plot no matter how inhomogeneous the structure.

#### CONCLUSIONS

- (1) The  $\beta$  diagram method of determining the axis of folding, although sound in theory, has very considerable limitations in practice, and is only serviceable if the folding is of homogeneous, cylindroidal type and shows a wide range of orientation of the planar structures; the angle of folding

must be from 40 degrees to 140 degrees and the folds must have rounded hinges (figure 11, type 2A). The method is imperfect when applied to homogeneous folds outside these limits (figure 11, types 1, 2B and 3) and is mathematically unsound if the folding is inhomogeneous.

- (2) The  $\pi$  diagram method of determining the axes of folds is a valuable one and, although with some sorts of folds (figure 11, types 1 and 3) there may be some difficulty in interpreting the results with precision, these difficulties may be overcome by certain modifications of the method.  $\pi$  diagrams provide much other information about a fold's geometry. In regions of inhomogeneous folding it is generally necessary to divide the data into more homogeneous sub-areas before accurate determinations of the fold direction may be made.

#### REFERENCES

- |                                 |      |  |
|---------------------------------|------|--|
| CLARK, R.H., and MCINTYRE, D.B. | 1951 | The use of the term pitch and plunge: Am. Jour. Sci., v.249, p.591-599.  |
| CLIFFORD, P.                    | 1960 | The geological structure of the Loch Luichart area, Ross-shire: Geol. Soc. London Quart. Jour., v.115, p.365-388.                    |
| FLEUTY, M.J.                    | 1962 | The three fold systems in the metamorphic rocks of upper Glen Orrin, Ross-shire: Geol. Soc. London Quart. Jour., v.117, p.447-476.   |
| JOHNSON, M.R.W.                 | 1957 | The structural geology of the Moine thrust zone in the Coulin Forest, Wester Ross: Geol. Soc. London Quart. Jour., v.113, p.241-270. |

- |                                 |        |   |
|---------------------------------|--------|---|
| KNOPF, E.B., and INGERSON E.    | 1938   | Structural Petrology: Geol. Soc. America Mem. 6.  |
| LINDSTRÖM, M.                   | 1960   | Methods of differentiating tectonic regimes: 21st Internat. Geol. Congress, part 18, p.347-352.                         |
| LINDSTRÖM, M.                   | 1961 a | On the significance of $\beta$ intersections in superposed deformation fabrics: Geol. Mag., v.98, No. 1, p.33-40.       |
| LINDSTRÖM, M.                   | 1961 b | Tectonic fabric of a sequence of areas in the Scandinavian Caledonides: Geol. Foreningens Forhandlingar, v.83, p.15-64. |
| PHILLIPS, F.C.                  | 1960   | The use of stereographic projection in structural geology:  |
| RAMSAY, J.G.                    | 1958 a | Superimposed folding at Loch Monar, Inverness-shire and Ross-shire: Geol. Soc. London Quart. Jour., v.113, p.271-308.   |
| RAMSAY, J.G.                    | 1958 b | Moine-Lewisian relations at Glenelg, Inverness-shire: Geol. Soc. London Quart. Jour., v.113, p.487-523.                 |
| SANDER, B.                      | 1948   | Einführung in die Gefügekunde der geologischen Körper: Springer-Verlag, Vienna & Innsbruck.                             |
| WEISS, L.E.                     | 1954   | A study of tectonic style: Univ. California Publ. Geol. Soc., v.30, No. 1, p.1-102.                                     |
| WEISS, L.E., and McINTYRE, D.B. | 1957   | Structural geometry of Dalradian rocks at Loch Leven, Scottish Highlands: Jour. Geol., v.65, p.575-602.                 |

## EXPLANATIONS TO FIGURES

- Fig. 1 The geometric principal used to determine the axis of folding by means of a  $\beta$  diagram. The lines of intersection of the bedding, axial plane and cleavage surfaces ( $\beta$  axes) are parallel to the fold axis  $f$ .
- Fig. 2 Determination of the angles  $\Psi_1$ ,  $\Psi_2$  and  $\Psi_3$  from three perpendicular reference axes for any  $\beta$  point.
- Fig. 3, and 4 Variation in the error ( $e_\beta$ ) in position of the  $\beta$  axis (stippled areas) which is produced by error ( $e_\pi$ ) in position of the bedding planes (poles A and B) at an angle  $d$  apart.
- Fig. 5 Variation in the maximum error in position of the calculated position of the  $\beta$  axis with variation in  $e_\pi$  and  $d$ .
- Fig. 6 Small circle (conical) zone of spurious  $\beta$  axes that may arise in a  $\beta$  diagram prepared from uniformly dipping surfaces (pole A) which are subject to an angular error in measurement of  $e_\pi$  degrees.
- Fig. 7  $\beta$  diagram prepared from a region with  $n$  fold systems ( $f_1, f_2, f_3, \dots, f_n$ ) of which  $c_1 \times$  surfaces are folded about  $f_1$ ,  $c_2 \times$  folded about  $f_2, \dots, c_n \times$  about  $f_n$ . In a  $\beta$  diagram made from all this data spurious  $\beta$  points ( $\beta_s$ ) will be developed by intersections of plane surfaces folded about axis  $f_1$  with those folded about  $f_2$ , etc.
- Fig. 8 Graphs showing the maximum percentage of significant  $\beta$  points in the total  $\beta$  synopsis with variation in  $n$  and  $c$ .
- Fig. 9 Graphs showing the minimum proportion of spurious  $\beta$  points to those  $\beta$  axes related to the least well developed fold system with variations in  $n$  and  $c$ .
- Fig. 10 The geometric principal used to determine the axis of folding by means of a  $\pi$  diagram. The normals to bedding surfaces at A, B, C and D ( $\pi_A, \pi_B, \pi_C$  and  $\pi_D$ ) and cleavage surface at E ( $\pi$ ) all lie on a plane or series of parallel planes normal to the fold axis  $f$ .

Fig. 11     $\beta$  diagrams and  $\pi$  diagrams prepared from different types of folds.

Fig. 12    A similar type fold with strata thinned on the limbs, showing the method of calculating the angles ( $\Phi$  and  $\Theta$ ) between the axial plane and the fold limbs using a  $\pi$  diagram.

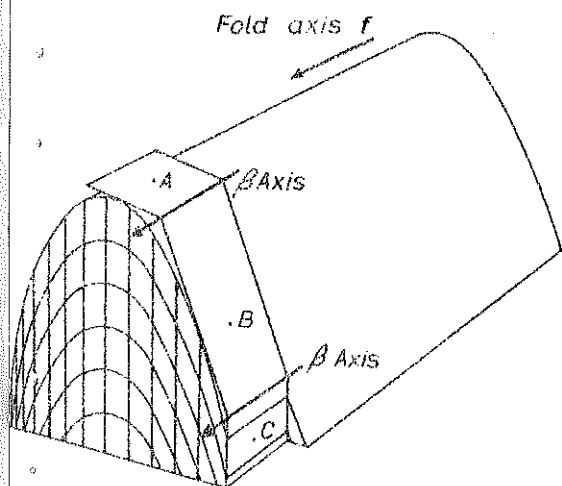


Figure 1

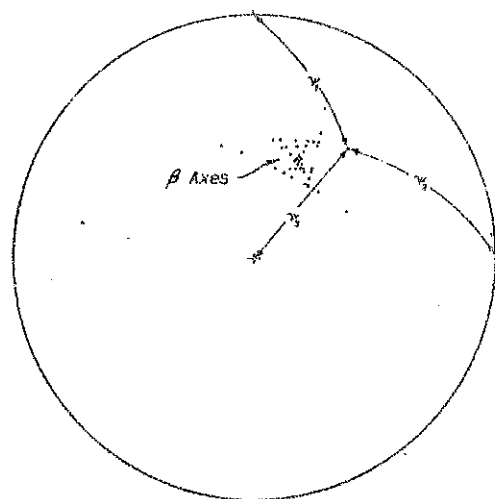


Figure 2

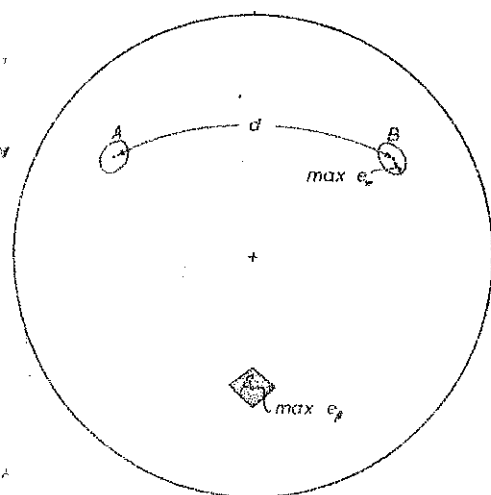


Figure 3

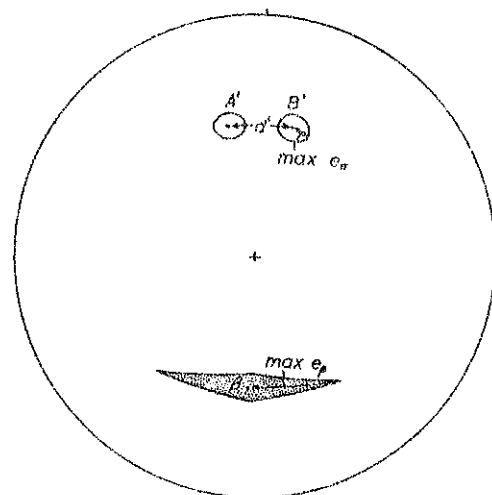


Figure 4



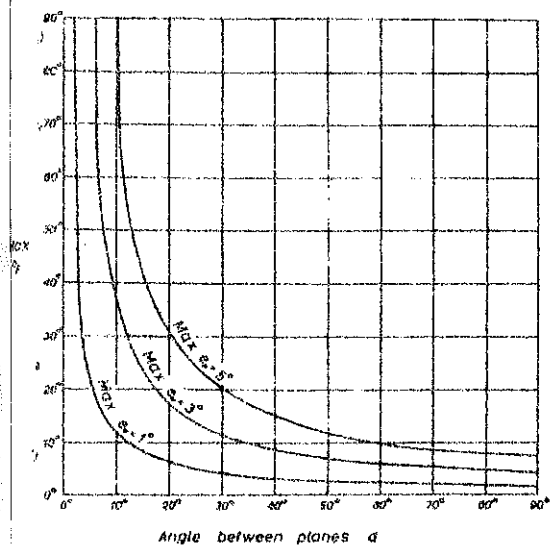


Figure 5

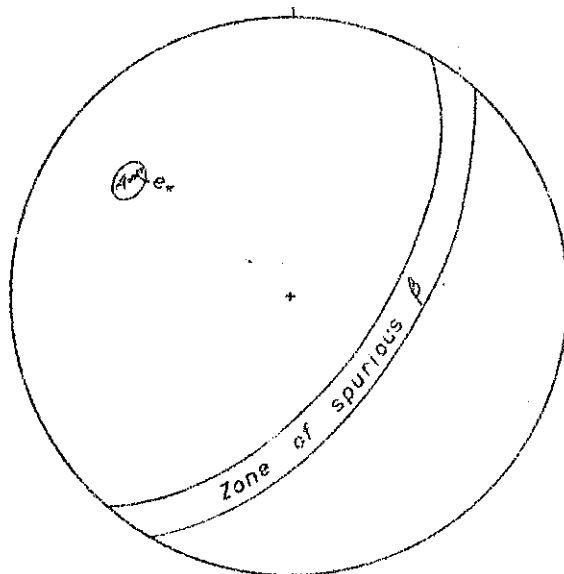


Figure 6

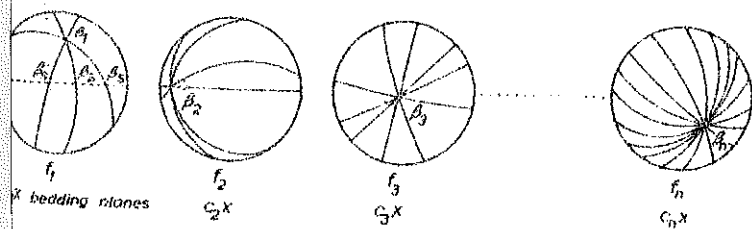


Figure 7

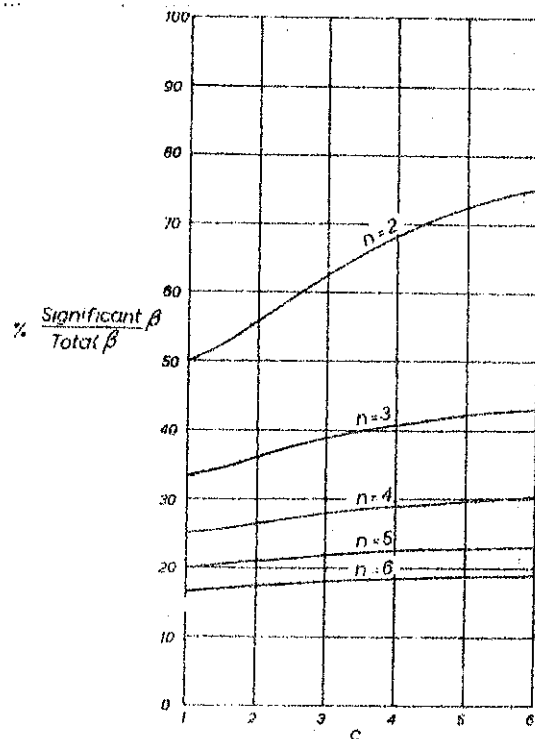


Figure 8

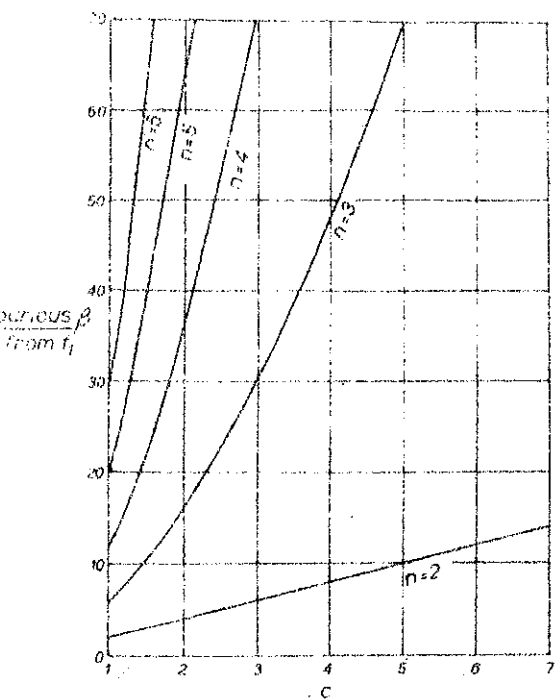


Figure 9

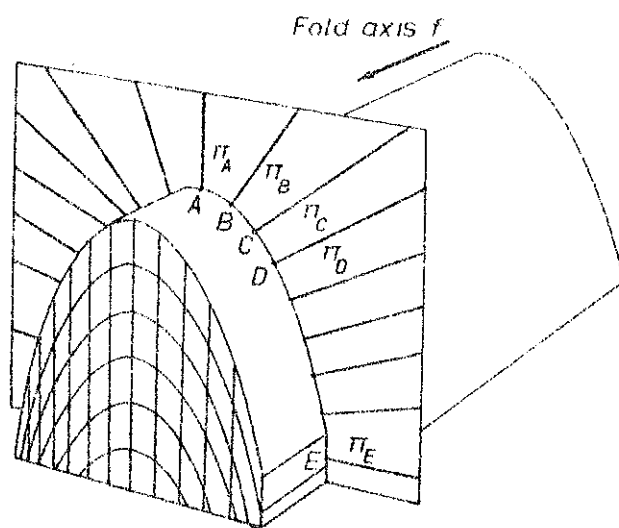
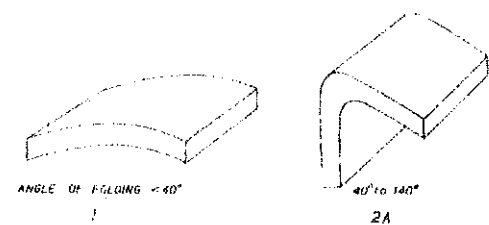


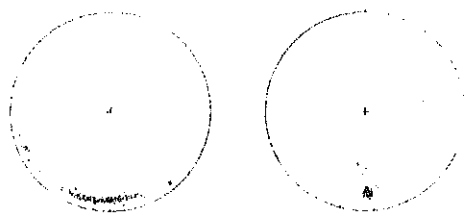
Figure 10

Figure 11

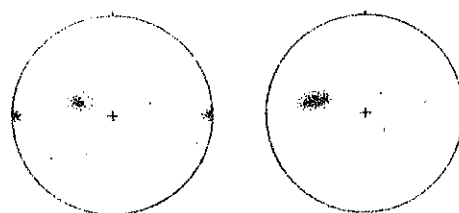
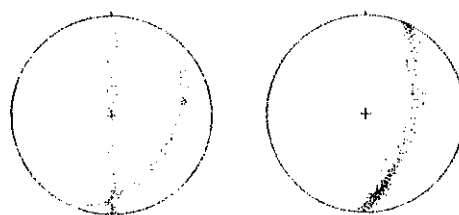
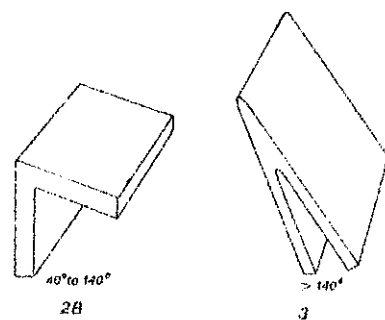
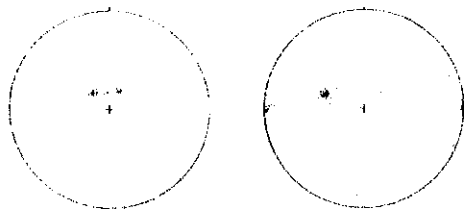
Types of folds



$\beta$  diagram analysis



$n$  diagram analysis



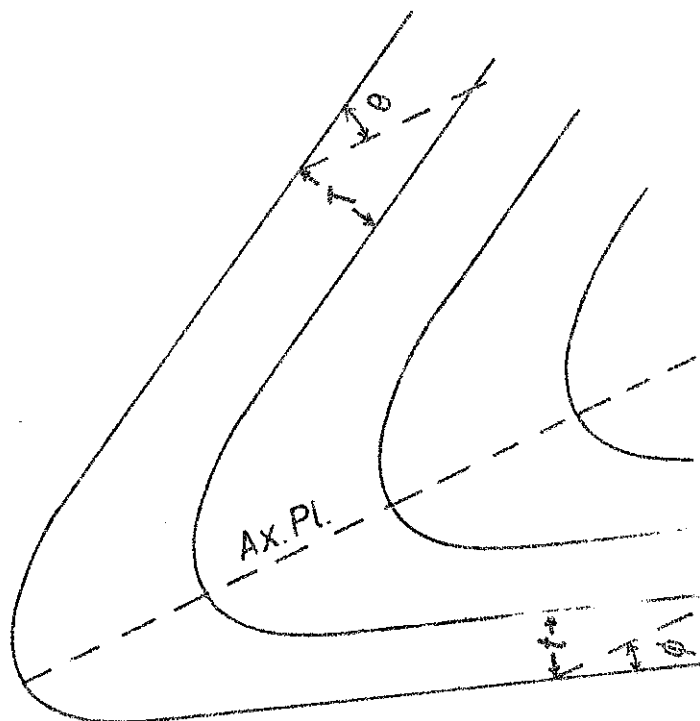
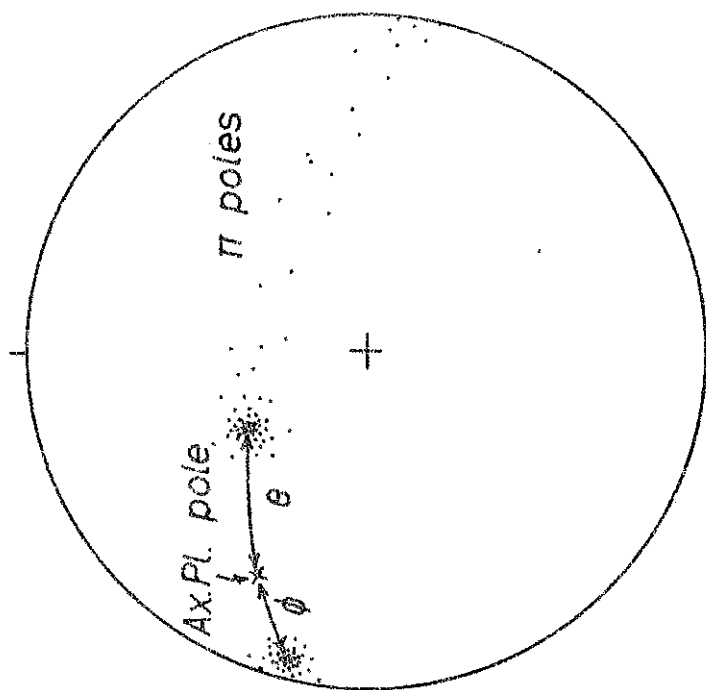


Figure 12